



Short Review

# Reaction mechanism of hydrogen activation by frustrated Lewis pairs

Lei Liu <sup>a,\*</sup>, Binit Lukose <sup>b</sup>, Pablo Jaque <sup>c</sup>, Bernd Ensing <sup>d</sup>

<sup>a</sup> Department of Physics & Earth Sciences, Jacobs University, Campus Ring 1, 28759 Bremen, Germany

<sup>b</sup> School of Electrical and Computer Engineering, Boston University, 02215 Boston, USA

<sup>c</sup> Department of Organic and Physical Chemistry, Faculty of Chemical and Pharmaceutical Sciences, University of Chile, Sergio Livingstone 1007, Santiago, Chile

<sup>d</sup> Van't Hoff Institute for Molecular Sciences, University of Amsterdam, 1098 XH Amsterdam, The Netherlands

Received 21 February 2018; revised 29 May 2018; accepted 6 June 2018

Available online 11 June 2018

## Abstract

Typically, a Lewis acid and a Lewis base can react with each other and form a classical Lewis adduct. The neutralization reaction can however be prevented by ligating the acid and base with bulky substituents and the resulting complex is known as a “frustrated Lewis pair” (FLP). Since the Lewis acid and base reactivity remains in the formed complex, FLPs can display interesting chemical activities, with promising applications in catalysis. For example, FLPs were shown to function as the first metal-free catalyst for molecular hydrogen activation. This, and other recent applications of FLPs, have opened a new thriving research field. In this short-review, we recapitulate the computational and experimental studies of the H<sub>2</sub> activation by FLPs. We discuss the thus-far uncovered mechanistic aspects, including pre-organization of FLPs, the reaction paths for the activation, the polarization of H–H bond and other factors affecting the reactivity. We aim to provide a rather complete mechanistic picture of the H<sub>2</sub> activation by FLPs, which has been under debate for decades since the first discovery of FLPs. This review is meant as a starting point for future studies and a guideline for industrial applications.

© 2018, Institute of Process Engineering, Chinese Academy of Sciences. Publishing services by Elsevier B.V. on behalf of KeAi Communications Co., Ltd. This is an open access article under the CC BY-NC-ND license (<http://creativecommons.org/licenses/by-nc-nd/4.0/>).

**Keywords:** Frustrated Lewis pairs; Hydrogen activation; Reaction mechanisms; Density functional theory; Molecular dynamics simulations

## 1. Introduction

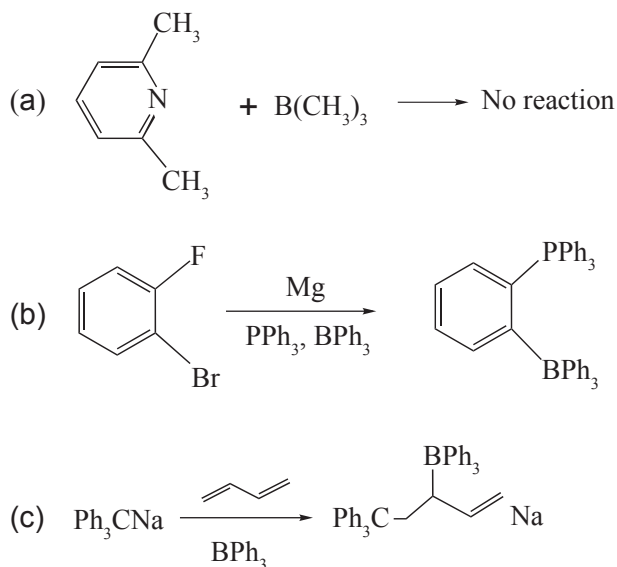
In 1923, Gilbert N. Lewis generalized a theory of acid-base reactions in which Lewis bases (LBs) are defined as molecules that are able to donate an electron pair, and Lewis acids (LAs) as molecules that are able to receive an electron pair. As the lowest unoccupied molecular orbital (LUMO) of the LAs interacts with the lone electron-pair in the highest occupied molecular orbital (HOMO) of the LBs, a stable Lewis acid-base adduct is formed (also called as classical Lewis adduct). This notion has become a primary axiom of chemistry, and a guiding principle in the understanding of chemical reactivity.

However, there are several exceptions that deviate from this Lewis axiom. The first example was reported by Brown and co-workers [1] upon studying the reactions between pyridines and various boranes. They found that while most of the LAs and LBs reacted with each other and formed classical Lewis adducts, the mixing of  $\alpha,\alpha'$ -lutidine with trimethylboron B(CH<sub>3</sub>)<sub>3</sub>, resulted in no reaction even at –80 °C (Scheme 1a) [2]. Steric hindrance between the *o*-methyl groups in  $\alpha,\alpha'$ -lutidine and the methyl groups in B(CH<sub>3</sub>)<sub>3</sub> was attributed to this behavior. This was the first study in which the term “steric hindrance” was used in Lewis acid and base chemistry. Another exception was later reported by Wittig and Benz [3], who did not observe formation of a classical Lewis adduct upon mixing of triphenylphosphine, PPh<sub>3</sub> (Lewis base, LB) with triphenylborane, BPh<sub>3</sub> (Lewis acid, LA). Instead, the addition of *o*-fluorobromobenzene to the above mixture yielded the *o*-phenylenebridged phosphonium-borate (Scheme

\* Corresponding author.

E-mail address: [liulei3039@gmail.com](mailto:liulei3039@gmail.com) (L. Liu).

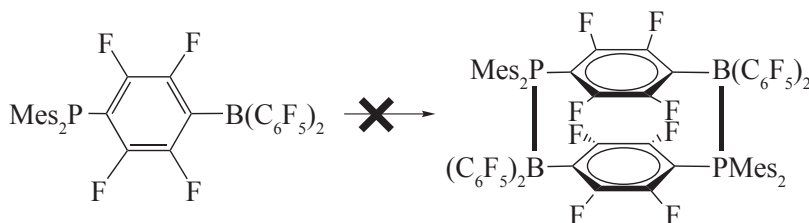
<sup>1</sup> Max Planck Institute for Polymer Research, Ackermannweg 10, 55128 Mainz, Germany.



Scheme 1. Three examples of non-quenched Lewis pairs: (a) Addition of trimethylboron to  $\alpha, \alpha'$ -lutidine leads to no reaction. (b) Reaction of *o*-fluorobromobenzene with the mixture of triphenylphosphine and triphenylborane. (c) Addition of triphenylborane to the butadiene monomer/triphenylmethane anion mixture.

1b). A similar phenomenon was observed by Tochtermann upon the addition of  $\text{BPh}_3$  to a butadiene monomer/triphenylmethane anion mixture. Instead of a classical Lewis adduct, a trapped product was obtained upon the addition of  $\text{BPh}_3$  and  $\text{Ph}_3\text{CNa}$  to butadiene (Scheme 1c) [4]. Both researchers realized that the bulky Lewis pairs prevent the formation of classical Lewis adducts, and Tochtermann used the German term “antagonistisches Paar” to describe such a non-quenched Lewis pair [4].

The term “frustrated Lewis pair” (FLP) was initially proposed by Stephan and co-workers in 2006 [5]. In their study, they reported a covalently linked phosphino–borane  $\text{Mes}_2\text{P}(\text{C}_6\text{F}_4)\text{B}(\text{C}_6\text{F}_5)_2$ . In solution, this phosphino–borane exists as a monomer since both the B and the P centers are sterically hindered, which precludes the dimerization or higher aggregation (Scheme 2). On the other hand, this molecule contains both LA and LB fragments, and therefore it has been classified as an FLP. More importantly, it has been shown that FLPs not only retain the typical reactivity of their individual components, but also exhibit a cooperative action of Lewis



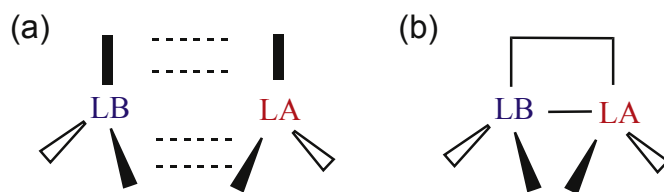
Scheme 2.  $\text{Mes}_2\text{P}(\text{C}_6\text{F}_4)\text{B}(\text{C}_6\text{F}_5)_2$ : the first example of a frustrated Lewis pair. Mes = 1,3,5-trimethylbenzene.

acid-base character owing to the presence of both reactive sites. Thus, these bifunctional systems emerge as potential metal-free catalysts with interesting applications in various chemical processes, which are typically achieved by transition metal-based catalysts. The applications include, activation of the H–H bond (molecular hydrogen) [5,6], capture of greenhouse gases (e.g.  $\text{CO}_2$  [7,8],  $\text{N}_2\text{O}$  [9], and  $\text{SO}_2$  [10]) and reduction of  $\text{CO}_2$  [11,12] imines [13–15] and many other unsaturated substrates. These metal-free and green catalytic systems have attracted an immense interest from researchers and, with that, FLP chemistry has become an active research focus [16]. There are several review papers in the literature summarizing studies of the FLP chemistry [17–26]. In this short-review, we focus on the studies which address the nature of hydrogen activation by FLPs, that is, the process of heterolytic splitting of  $\text{H}_2$  into a proton ( $\text{H}^+$ ) and a hydride ( $\text{H}^-$ ) in the presence of either intra- or intermolecular FLPs.

## 2. Reaction mechanism of $\text{H}_2$ activation by FLPs

### 2.1. Preorganization of FLPs

In general, there are two types of FLPs classified according to their electronic structures. The first type is the intermolecular FLPs, in which the LA and LB centers are contained in two separate molecules (Scheme 3a) [27]. For this type of FLPs, it is assumed that when brought into contact in solution, the two individual components (LA and LB) associate into a loosely bound complex through secondary interactions mainly London dispersion interactions [28,29], which then interacts with incoming small molecules, e.g.  $\text{H}_2$ ,  $\text{CO}_2$  and  $\text{SO}_2$ . However, early experimental attempts could not observe the formation of such complexes. For example, the resonance signals



Scheme 3. Schematic representation of two types of FLPs: (a) intermolecular FLPs and (b) intramolecular FLPs. Notation used: LA for Lewis acid, LB for Lewis base.

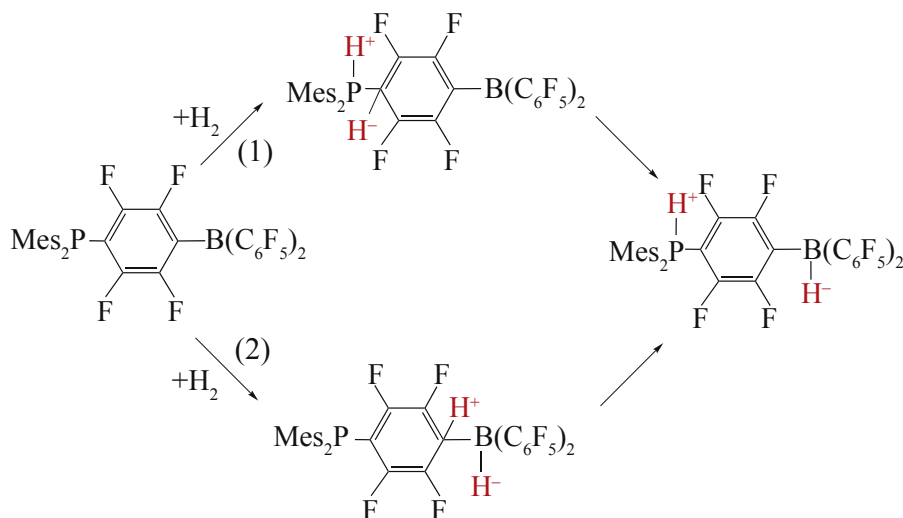
in NMR measurements of the FLP mixture were found to be identical to those of the individual components [6]. The yellow color of the  $t\text{Bu}_3\text{P}/\text{B}(\text{C}_6\text{F}_5)_3$  mixture was thought to arise from the bound complex [6,30], but a later experimental mechanistic study indicated that the color is characteristic of the  $t\text{Bu}_2\text{PC}_6\text{F}_4\text{B}(\text{C}_6\text{F}_5)_2$  compound formed during the mixing of  $t\text{Bu}_3\text{P}$  and  $\text{B}(\text{C}_6\text{F}_5)_3$  [31]. Later, several advanced experimental techniques were employed to investigate the associations of the LA/LB mixture. Typical examples are: Wiegand et al. discovered that it is possible to distinguish between classic Lewis adducts and FLPs through a solid-state NMR method [32]. By means of Nuclear Overhauser Effect Spectroscopy (NOESY) measurements, Rocchigiani et al. found that the association of  $\text{PMe}_3/\text{B}(\text{C}_6\text{F}_5)_3$  into a FLP is slightly endergonic ( $\Delta G = 0.4 \text{ kcal mol}^{-1}$ ) [33]. Nevertheless, the molecular level details of the association of the LA/LB fragments remained unclear. The electronic structures of the loosely bound FLPs could thus far only be probed computationally by means of Density Functional Theory (DFT) calculations [28,29,34–37]. With electronic energy and solvent effects considered, the FLP complexes are found to be more stable than the separate components, with an average association energy ( $\Delta E_{\text{solv}}$ ) of  $-10 \text{ kcal mol}^{-1}$  [36]. When entropy effects are also taken into account, the stability of the FLP complexes is seen to be somewhat reduced, and the computed association Gibbs free energies ( $\Delta G_{\text{solv}}$ ) of formation are reported at  $5 \text{ kcal mol}^{-1}$  [36],  $2 \text{ kcal mol}^{-1}$  and  $0 \text{ kcal mol}^{-1}$  at various levels of theory [28]. Interestingly, a molecular dynamics (MD) simulation study showed that the association of the two components spontaneously occurs, leading to the formation of intermolecular FLPs, although the probability to find such an FLP complex is low with only 2% of the total amount of phosphine and borane molecules being complexed in the simulations [38]. Considering proper orientation of the reactive centers, the concentration of reactive FLP complexes is even lower, at only 0.5%. Although the probability to form FLPs is low,  $\text{H}_2$  can be activated by FLPs at a micromolar level. Based on the constrained potential energy surface (PES) scan with respect to the distance between the LA (boron atom, B) and the LB (phosphorus atom, P) centers ( $d_{\text{PB}}$ ), it was found that the optimal  $d_{\text{PB}}$  for active intermolecular FLPs is ranged between 3 Å and 5 Å [36]. When the substituent groups attached to the reactive centers are too bulky and the repulsive interactions between the two components are too large, the  $d_{\text{PB}}$  is very long (i.e.  $d_{\text{PB}}$  is more than 5 Å for  $t\text{Bu}_3\text{P}/\text{BMe}_3$ ) [36]. This leads to inactive FLPs, which cannot be used for activation of  $\text{H}_2$  or other small molecules [6]. On the other hand, when the substituents are too small, then the LAs react with the LBs, thus favoring the formation of classic Lewis adducts (i.e.  $\text{Me}_3\text{P}/\text{B}(\text{C}_6\text{F}_5)_3$ ,  $\text{Me}_3\text{P}/\text{B}(\text{C}_6\text{F}_4\text{H})_3$  and  $\text{TMP}/\text{BH}(\text{C}_6\text{F}_5)_2$ ). [6,39,40] It is important to point out that the shape of the constrained PES plays a significant role in the activity of FLPs as well. In particular in the case of a flat PES, the two components can easily move without having to overcome any significant energy barrier, and they may thus form an active FLP in which the minimum  $d_{\text{PB}}$  is not in the optimal range ( $3 \text{ Å} < d_{\text{PB}} < 5 \text{ Å}$ ).

The second FLP type is the intramolecular FLPs, where the LA/LB components are connected through a covalent C–C bridge and thus they are part of a single molecule (Scheme 3b) [41]. Unlike intermolecular FLPs, in which LA/LB centers are associated by weak LA/LB interactions, the reactive centers in intramolecular FLPs are covalently connected to each other, with LA–LB distances that resemble that of the classic Lewis adducts. Taking the typical intramolecular FLP,  $\text{Mes}_2\text{P}(\text{CH}_2)_2\text{B}(\text{C}_6\text{F}_5)_2$ , as an example: the most stable structure is a four-membered heterocyclic phosphane–borane adduct, and the  $d_{\text{PB}}$  is 2.2 Å [42]. To form an intramolecular FLPs and to activate  $\text{H}_2$ , first the closed ring structure need to open. Energy is needed to break the interactions between P and B, and to increase the  $d_{\text{PB}}$  from 2.2 Å to an ideal distance. DFT calculations predict an open structure with a  $d_{\text{PB}}$  of 2.8 Å, which lies  $7 \text{ kcal mol}^{-1}$  above the closed structure on the PES. It is believed that such an open form is responsible for the  $\text{H}_2$  activation [42]. Similar results have been found for a series of intramolecular FLPs where all open structures are  $10 \text{ kcal mol}^{-1}$  less stable than the closed forms [43], revealing that the LA–LB dissociation of many intramolecular FLPs is thermodynamically mildly endergonic. Moreover, it was found that the energy barriers for this opening-process (or pre-equilibration step) are also low [44]. To form intramolecular FLPs, the interactions between the LA/LB centers should not be too strong, otherwise too much energy is needed to form open structures, rendering the FLPs inactive. In other words, the strength of LA/LB should be moderate, which can be tuned by the substituents on both reactive centers. Moreover, Erker et al. pointed out that geometric parameters and conformational flexibility are also of great importance [45]. Rigid LA/LB frameworks are expected to have a reduced reactivity towards  $\text{H}_2$  and other small molecules.

## 2.2. Reaction path for $\text{H}_2$ activation by FLPs

The first study on the reaction path of  $\text{H}_2$  activation by FLPs has been reported by Stephan and co-workers [5]. The injection of  $\text{H}_2$  into the solution of  $\text{Mes}_2\text{P}(\text{C}_6\text{F}_4)\text{B}(\text{C}_6\text{F}_5)_2$  at  $25^\circ\text{C}$  resulted in rapid generation of a zwitterionic salt,  $[\text{Mes}_2\text{PH}]^+(\text{C}_6\text{F}_4)[\text{BH}(\text{C}_6\text{F}_5)_2]^-$ , during which the solution color changed from orange to colorless. Heating this salt to  $150^\circ\text{C}$  led to release of  $\text{H}_2$  and then regeneration of the FLP back into the phosphino–borane reactant (Scheme 2). This remarkable finding represented the first transition metal free system that activates  $\text{H}_2$  reversibly. In that study, the authors proposed two possible reaction paths for  $\text{H}_2$  activation by  $\text{Mes}_2\text{P}(\text{C}_6\text{F}_4)\text{B}(\text{C}_6\text{F}_5)_2$ . One pathway is the addition of  $\text{H}_2$  to the P–C bond, followed by hydride migration from the C atom to the B atom. The other pathway is the addition of  $\text{H}_2$  to the B–C bond, followed by proton migration from the C atom to the P atom (Scheme 4).

Later, on the basis of DFT calculations, Guo et al. [46] proposed an alternative path for the reaction between  $\text{H}_2$  and  $\text{Mes}_2\text{P}(\text{C}_6\text{F}_4)\text{B}(\text{C}_6\text{F}_5)_2$ . The authors explored and compared three possible pathways: (1) a hydride migration pathway; (2)



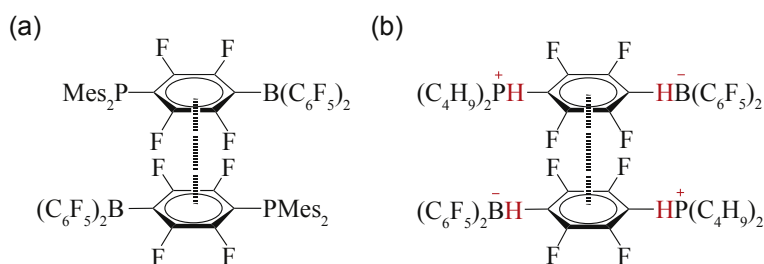
Scheme 4. Two possible reaction pathways for the reversible hydrogen activation by  $\text{Mes}_2\text{P}(\text{C}_6\text{F}_4)\text{B}(\text{C}_6\text{F}_5)_2$ : (1) hydride migration, and (2) proton migration. Mes = 1,3,5-trimethylbenzene.

a proton migration pathway; and (3) a concerted Lewis acid-base pathway. Their findings indicate that the concerted Lewis acid-base pathway, which involves  $\pi$ - $\pi$  stacking of two  $\text{Mes}_2\text{P}(\text{C}_6\text{F}_4)\text{B}(\text{C}_6\text{F}_5)_2$  molecules (Scheme 5a), has a lower energy barrier in the rate-limiting step than that of the two migration mechanisms, which were proposed by Stephan et al. ( $33.7 \text{ kcal mol}^{-1}$  versus  $69.1$  and  $54.7 \text{ kcal mol}^{-1}$ ) [5]. In this concerted reaction path, the two reactive centers (B and P) are from two distinct  $\text{Mes}_2\text{P}(\text{C}_6\text{F}_4)\text{B}(\text{C}_6\text{F}_5)_2$  molecules. As such, the  $\text{H}_2$  activation proceeds actually through an intermolecular catalysis. A key step for this pathway is the dimerization of the two  $\text{Mes}_2\text{P}(\text{C}_6\text{F}_4)\text{B}(\text{C}_6\text{F}_5)_2$  molecules. The experimental findings of Welch et al. [47] regarding the crystal structure of the hydrogenated product,  $[(\text{C}_4\text{H}_9)_2\text{PH}]^+(\text{C}_6\text{F}_4)[\text{BH}(\text{C}_6\text{F}_5)_2]^-$ , is in support of the dimerization pathway. They found that the monomers pack in pairs, in a head-to-tail manner, with a short  $\text{H}^{\delta+} \cdots \text{H}^{\delta-}$  distance of  $2.6 \text{ \AA}$  (Scheme 5b).

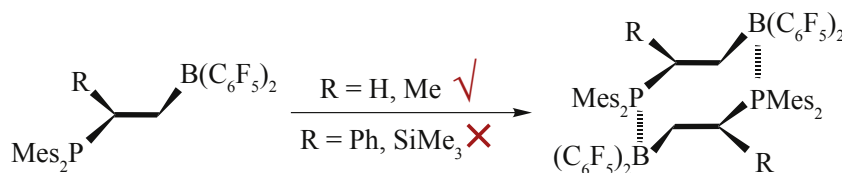
Similar to that work, Liu et al. [48] reported computational studies of  $\text{H}_2$  activation by a series of intramolecular FLPs,  $\text{Mes}_2\text{PCHRCH}_2\text{B}(\text{C}_6\text{F}_5)_2$ , with  $R = \text{H}$ , Me, Ph, and  $\text{SiMe}_3$ . These FLPs showed different reactivities towards  $\text{H}_2$ : in the cases of  $R = \text{H}$  and Me, the FLPs show  $\text{H}_2$  activation, whereas in the cases of  $R = \text{Ph}$  and  $\text{SiMe}_3$ , the FLPs are inactive towards  $\text{H}_2$  [49]. The reaction paths that were known in the

literature, which assumed a bimolecular reaction between the open FLP conformers and  $\text{H}_2$  [34,35], were not able to explain the experimentally observed different reactivities towards  $\text{H}_2$ . The authors showed that the dimerization of FLPs is possible for less bulky substituents, i.e. H and Me. However, this is not possible in the presence of bulky substituents like Ph or  $\text{SiMe}_3$ , and the reaction path becomes inaccessible because of the extra steric hindrance on the C–C bridge (Scheme 6) [48]. Hence, this reaction path gives an adequate explanation for the selective reactivity towards  $\text{H}_2$ .

However, the reaction path that involves dimerization of FLPs is somehow in contrast to the experimental observations. The following examples illustrate that: Stephan et al. [5] performed kinetic studies using  $^{31}\text{P}$  ( $^1\text{H}$ ) NMR spectroscopy to gain deeper insight into the reaction. The derived data showed that the reverse reaction (release of  $\text{H}_2$ ) is first-order in terms of the concentration of  $[\text{Mes}_2\text{PH}]^+(\text{C}_6\text{F}_4)[\text{BH}(\text{C}_6\text{F}_5)_2]^-$ . Recent kinetic studies on other FLP systems also revealed that  $\text{H}_2$  activation by a series of FLPs is first-order in  $[\text{PH}]^+ / [\text{BH}]^-$  species [50,51]. Moreover, theoretical studies on the  $\text{H}_2$  activation by FLPs indicate that the dimerization of FLPs is unnecessary to explain the reactivities of FLPs with  $\text{H}_2$ . Based on *ab initio* and DFT calculations, Rajeev et al. reexamined the  $\text{H}_2$  activation by  $\text{Mes}_2\text{P}(\text{C}_6\text{F}_4)\text{B}(\text{C}_6\text{F}_5)_2$  using a simplified



Scheme 5. The intermolecular  $\pi$ - $\pi$  stacking of (a) two  $\text{Mes}_2\text{P}(\text{C}_6\text{F}_4)\text{B}(\text{C}_6\text{F}_5)_2$  molecules, and (b) two  $[(\text{C}_4\text{H}_9)_2\text{PH}]^+(\text{C}_6\text{F}_4)[\text{BH}(\text{C}_6\text{F}_5)_2]^-$  zwitterionic salt units. Mes = 1,3,5-trimethylbenzene.



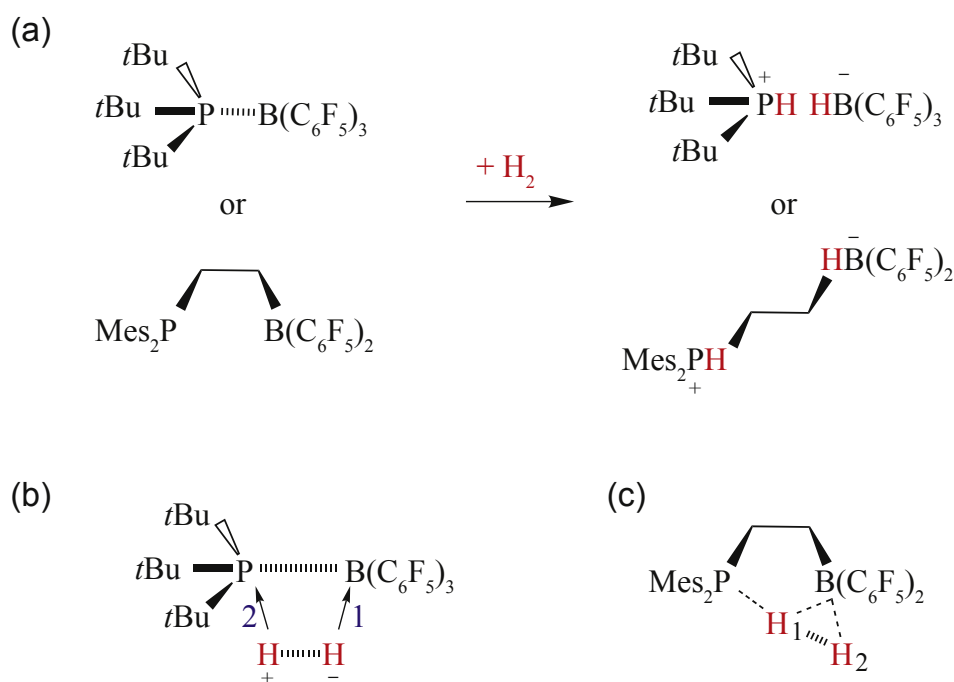
Scheme 6. The intermolecular stacking of two open conformers of  $\text{Mes}_2\text{PCHRCH}_2\text{B}(\text{C}_6\text{F}_5)_2$ , with  $R = \text{H}, \text{Me}$  and  $R = \text{Ph}, \text{SiMe}_3$ . Mes = 1,3,5-trimethylbenzene. Note that in the case of  $R = \text{SiMe}_3$ , the substituent group is attached to the bridging C atom connected to B atom.

model system,  $(\text{CH}_3)_2\text{P}(\text{C}_6\text{F}_4)\text{B}(\text{CF}_3)_2$  [52]. The calculations showed that the reaction path, which involves a series of rearrangement reactions such as proton or hydride migration (Scheme 4) is both thermodynamically and kinetically feasible. In addition, the computed reaction Gibbs free energies are in good agreement with the experimental observations, i.e.  $\text{H}_2$  activation occurs at room temperature and the reverse liberation process happens at an elevated temperature (150 °C). On the other hand, the highest energy barrier along the lowest energy path was found to be circa 30 kcal mol<sup>-1</sup>, which agrees with the reactions taking place at finite temperature.

It is commonly accepted that the reaction path for  $\text{H}_2$  activation by FLPs is a bimolecular step involving  $\text{H}_2$  and FLP, without the need for the dimerization of two FLP molecules. According to DFT calculations, the FLP and  $\text{H}_2$  reactants and the hydrogenation product ( $[\text{LBH}]^+[\text{LAH}]^-$ ) are connected through only one transition state (TS), and the  $\text{H}_2$  activation by the FLP follows a concerted reaction path for both inter- and intramolecular FLPs (Scheme 7a). When  $\text{H}_2$  interacts with FLPs, the H–H bond is polarized by the cooperative action of

the LA/LB centers. After the heterolytic splitting of the H–H bond, the proton and the hydride are synchronously or asynchronously captured by the LA and LB. Based on this DFT reaction path model, the computed energy barrier for  $\text{H}_2$  activation by the prototypical intramolecular FLP,  $\text{Mes}_2\text{P}(\text{CH}_2)_3\text{MeB}(\text{C}_6\text{F}_5)_2$ , is in perfect agreement with the experimentally measured values. The DFT (B2PLYP-D3/def2-QZVP (COSMO-RS, dichloromethane)//TPSS-D3/def2-TZVP) calculated energy barrier is 20.7 kcal mol<sup>-1</sup>, which is in very good agreement with the experimental value of 22.3 kcal mol<sup>-1</sup>. Moreover, the reaction rates displays a kinetic isotope effect of  $k_{\text{HH}}/k_{\text{DD}}$  equal to 3.19 in the experiment while the computed value is 3.24 [51].

More recently, the detailed reaction path for  $\text{H}_2$  activation by FLPs has been investigated by *Ab Initio* Molecular Dynamics (AIMD) simulations [53–56]. These simulations confirmed the general picture already established by static DFT calculations: the stoichiometric ratio of FLP to  $\text{H}_2$  is equal to one and the dimerization of two FLP molecules is unnecessary. Interestingly, the MD simulations showed that the process of  $\text{H}_2$  activation by FLPs consists of two steps



Scheme 7. (a) Concerted mechanisms for  $\text{H}_2$  activation by inter- and intramolecular FLPs obtained by DFT calculations. (b) Two-step mechanism for  $\text{H}_2$  activation by an intermolecular FLP, obtained by AIMD. (c) TS for  $\text{H}_2$  activation by an intramolecular FLP obtained by DFT calculations.  $t\text{Bu} = \text{tert-butyl}$ . Mes = 1,3,5-trimethylbenzene.



(Scheme 7b): after polarization of  $H_2$ , the hydride is first captured by the Lewis acid (B), and then the proton is captured by the Lewis base (P/N). Actually, such a two-step reaction mechanism had already been suggested indirectly from static DFT calculations. At the TS of the  $H_2$  activation by the intermolecular FLP,  $tBu_3P/B(C_6F_5)_3$ , a single imaginary frequency shows that the hydride interacts stronger with the LA center than the proton with the LB center. The B–H distance is considerable shorter than the P–H distance (1.68 Å versus 2.10 Å), and the computed covalent bond orders indicate that the B–H bond is formed prior to the P–H bond [35]. In addition, DFT calculations on  $H_2$  activation by an intramolecular FLP,  $Mes_2P(CH_2)_3MeB(C_6F_5)_2$ , show that the  $H_1 \cdots H_2$  fragment has a side-on arrangement to B and, at the same time, an almost linear arrangement of the  $P \cdots H_1 \cdots H_2$  moiety (Scheme 7c). The single imaginary frequency indicates that  $H_2$  is activated at the B center, followed by the P atom pulling the proton from the activated hydrogen molecule [51].

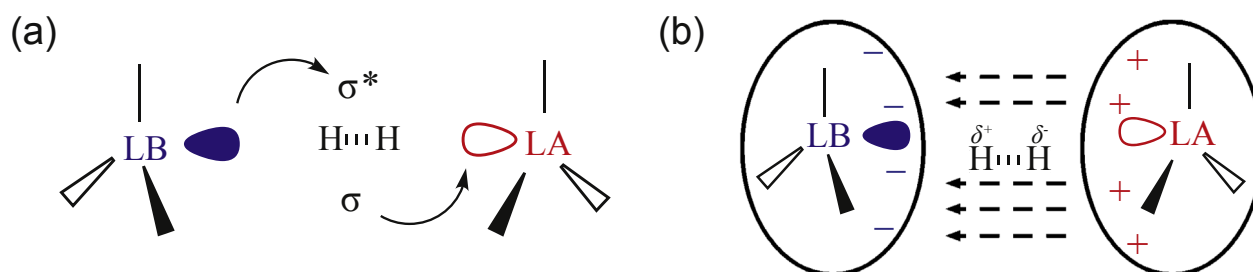
### 2.3. Polarization of H–H bond

So far, two DFT based models that explain the polarization of H–H bonds have been proposed in the literature. The first one, the electron transfer (ET) model, was proposed by Pápai et al. [34], who assumed that the LA/LB parts initially associate to form a weakly bound pair (also called “encounter complex”), which then interacts with  $H_2$ , and polarizes it in a concerted manner. A detailed molecular-orbital analysis [57] indicated that a simultaneous electron transfer from the lone pair of  $tBu_3P$  to  $\sigma^*(H_2)$  and from  $\sigma(H_2)$  to the empty p orbital of  $B(C_6F_5)_3$  occurs in a push–pull manner (Scheme 8a), and results in weakening and subsequent heterolytic cleavage of the dihydrogen bond. In the TS structure,  $H_2$  occupies the reactive pocket of the P/B pair in an almost linear P–H–B arrangement with a slightly elongated H–H distance of 0.79 Å. The computed imaginary frequency corresponds to the stretching of the H–H bond and the formation of P–H and B–H bonds. The reaction barrier was associated with the energy cost for creating the orbital overlaps and distorting the individual donor and acceptor molecules [57].

An alternative and simpler mechanistic picture of the FLP-driven  $H_2$  activation was later proposed by Grimme and co-workers, which is the so-called electric field (EF) model [35]. It also assumes that a weakly bound pair is formed

between the LA/LB parts through noncovalent secondary interactions (i.e. dispersion effects and hydrogen bonds). The incoming  $H_2$  is then polarized and later split by the electric field created by the FLP (Scheme 8b). The computed imaginary frequency corresponds to the stretching of the H–H bond and the entrance of the  $H_2$  molecule into the FLP pocket. The EF model suggests that the most uphill step is the entrance of the  $H_2$  molecule into the FLP cavity, afterwards the reaction proceeds in a barrier-less manner, and there is no need to consider specific  $H_2$ /FLP orbital interactions.

It should be noted that there is still some debate over these two models. On the one hand, the EF model for  $H_2$  activation was reinvestigated with several DFT and full CI studies [58]. All methods showed that the activation barrier is strongly dependent on the electric field, which drastically decreases as the electric field strength increases. The barrier even disappears at strong (but experimentally accessible) electric fields. This investigation supported the original EF model, in which the key step is the polarization of the hydrogen molecule. On the other hand, there are several studies supporting the ET model. For example, by investigating the reactions between simple Lewis pairs ( $NH_3 + BX_3$ ,  $X = H, F, Cl$ ) and  $H_2$ , Camaioni et al. [59] found that the EF created by the  $NH_3/BX_3$  pair indeed has a polarizing effect, but its contribution is so small that it cannot cleave the hydrogen molecule. Later, the ET and EF models were thoroughly compared by examining a set of representative  $H_2$  activation reactions [60]. The results showed that the EF model has several shortcomings while the ET model could provide a better understanding on the main features of the  $H_2$  activation reactions. However, a recent MD simulation study revealed that these two models are somehow complementary to each other [56]. For example, when  $H_2$  is far away from the reactive centers, with a distance larger than 2.5 Å, the H–H bond is polarized mainly through the electric field created by the FLPs. At such a large distance, the  $H_2$  already becomes polarized, and the average H–H distance is 0.8 Å. Analysis of the electron density difference did not show significant electron transfer between  $H_2$  and the FLP molecules. When  $H_2$  gets closer than 2.5 Å to the LA/LB centers, the electron density difference clearly shows electron transfer from  $H^-$  to B and from P to  $H^+$ . In other words, the ET model is the most fitting model for the polarization of H–H bond in the short distance region, but the EF model may apply in that region as well. More recently, on the basis of the activation



Scheme 8. Schematic representation of (a) the electron-transfer (ET) model of Pápai et al. [34] and (b) the electric-field (EF) model of Grimme et al. [35] Notation used: LA for Lewis acid, LB for Lewis base.

strain model (ASM) combined with EDA-NOCV analysis (energy decomposition analysis with natural orbital chemical valence theory), Yepes et al. [61] showed that a kinetically feasible H–H bond activation is driven by asynchronous orbital interactions in germinal aminoborane-based FLPs.

#### 2.4. Factors affecting reactivity

Several reports have shown that intramolecular FLPs often show greater reactivity than their intermolecular counterparts [62,63]. This is most likely due to the fact that intramolecular FLPs do not have association bottlenecks, as both LA/LB reactive centers are already bound at the same backbone. Therefore, the possibility to form intramolecular FLPs is much higher than that of intermolecular FLPs in solution. For both types of FLPs, the reaction thermodynamics with H<sub>2</sub> are strongly affected by the cumulative strength of the LA/LB parts, which can be quantified by the proton affinity and hydride affinity [64]. For example, it was found that FLPs could show different reactivity with H<sub>2</sub> by changing the substituents on the LA/LB centers (Table 1): *t*Bu<sub>3</sub>P + B(*p*-C<sub>6</sub>F<sub>4</sub>H)<sub>3</sub> (FLP 1) and Mes<sub>3</sub>P + B(C<sub>6</sub>F<sub>5</sub>)<sub>3</sub> (FLP 2) showed non-reversible H<sub>2</sub> activation [6,65] (*o*-C<sub>6</sub>H<sub>4</sub>Me)<sub>3</sub>P + B(*p*-C<sub>6</sub>F<sub>4</sub>H)<sub>3</sub> (FLP 3) showed reversible H<sub>2</sub> activation [65], and (C<sub>6</sub>F<sub>5</sub>)<sub>3</sub>P + B(C<sub>6</sub>F<sub>5</sub>)<sub>3</sub> (FLP 4) showed no reaction with H<sub>2</sub> in solution [6]. Based on DFT and *ab initio* calculations, Vankova et al. [36] demonstrated that these different reactivities of FLP 1–4 can be explained by the cumulative strength of the LA/LB parts. The FLP 1 and FLP 2 contain either a strong acid, B(C<sub>6</sub>F<sub>5</sub>)<sub>3</sub>, or a strong base, *t*Bu<sub>3</sub>P. The reaction Gibbs free energies ( $\Delta G$ ) are largely negative, indicating that the zwitterionic products [(LBH)<sup>+</sup>(LAH)<sup>−</sup>] are very stable, and consequently it is difficult to liberate H<sub>2</sub>. The computed value of  $\Delta G$  is close to zero for FLP 3 containing a LA/LB pair with moderate strength. Therefore, this pair could, on the one hand, activate H<sub>2</sub>. On the other hand, the final product could relatively easily release H<sub>2</sub> upon heating the solution. The strength of FLP 4 is so weak that it cannot split the H–H bond and the reaction with H<sub>2</sub> shows a large positive  $\Delta G$  value. Such a relationship between reactivity and strength of FLPs has also been investigated by Tibor et al. [64] with quantum chemical calculations, by Rebecca et al. [66] and by Jiang et al. [67] with experimental techniques. Note that the cumulative acid-base strength not only determines the thermodynamic

balance of the overall H<sub>2</sub> activation process, but also shows a systematic effect on the kinetics. According to the DFT calculations by Liu et al. [68], increasing the strength of the LA/LB components in the FLPs decreases the energy barriers for H<sub>2</sub> activation. In other words, the stronger FLPs exhibit lower energy barriers for H<sub>2</sub> activation and led to highly stable zwitterionic salts in accordance to the Bell–Evans–Polanyi principle [69,70]. A similar trend has also been found by Yepes et al. based on the theoretical investigation of H<sub>2</sub> activation by several germinal aminoborane-based intramolecular FLPs [61].

The thermodynamics of the H<sub>2</sub> activation by FLPs is also strongly affected by the environment, which is usually an organic solvent. Grimme et al. [20] pointed out that it is important to include the solvation free energies ( $\delta G_{\text{solv}}$ ) when computing  $\Delta G$ , and it was shown that solvent contributions are around  $-10 \text{ kcal mol}^{-1}$  according to COSMO-RS (conductor-like screening model for realistic solvents) calculations. Recently, a study was carried out to gain a deeper insight into the reactivity of several intramolecular FLPs, Mes<sub>2</sub>P(CH<sub>2</sub>)<sub>n</sub>B(C<sub>6</sub>F<sub>5</sub>)<sub>2</sub>, towards H<sub>2</sub> (Table 1 FLPs 5–7) [43]. The DFT results showed that H<sub>2</sub> activation is kinetically feasible by all of these FLP systems since all computed energy barriers were less than  $15 \text{ kcal mol}^{-1}$ . The authors concluded that the experimentally obtained different reactivity of FLPs 5–7 towards H<sub>2</sub> is mainly because of their thermodynamics. The overall H<sub>2</sub> activation by the inactive FLP is endergonic ( $8.6 \text{ kcal mol}^{-1}$  for FLP 6), while it is slightly endergonic ( $1.5 \text{ kcal mol}^{-1}$  for FLP 7) or exergonic ( $-7.5 \text{ kcal mol}^{-1}$  for FLP 5) for the reactive FLPs. When  $\Delta G$  was partitioned into gas-phase Gibbs free energies,  $\Delta G_{\text{gas}}$ , and solvation free energies,  $\delta G_{\text{solv}}$ , three interesting observations were made: (1) the  $\delta G_{\text{solv}}$  is less than  $-13 \text{ kcal mol}^{-1}$  in all cases, which is the largest contribution (absolute values) when computing  $\Delta G$ . (2) all FLPs 5–7 cannot activate H<sub>2</sub> without the solvent contributions since all  $\Delta G_{\text{gas}}$  values are largely positive; (3) FLP 6 and FLP 7 have similar values for  $\Delta G_{\text{gas}}$  of about  $20 \text{ kcal mol}^{-1}$ . FLP 7 is reactive with H<sub>2</sub> because of the large solvent contributions ( $-18.5 \text{ kcal mol}^{-1}$ ), while  $\delta G_{\text{solv}}$  is only  $-13.6 \text{ kcal mol}^{-1}$  in the case of FLP 6, rendering it inactive. The role of solvent is not only limited to H<sub>2</sub> activation, but also to other reactions of FLPs [71–74]. Interestingly, it was found that the crystal field could replace the solvation contributions when the reactivity of FLPs is transferred from solution to the solid state (i.e. in the form of a molecular crystal). Theoretical studies showed that the gas-phase reaction energies ( $\Delta E$ ) are always more negative in the solid state than in the gas and the solution phase for the same H<sub>2</sub> activation reactions [75].

It is believed that the LA/LB pair works in a cooperative fashion, for both the formation of the FLPs and the splitting of the H–H bond. However, the actual individual roles of the LA and LB remained unclear: that is whether both components are equally important to the thermodynamics and kinetics of the catalytic activity. To answer this fundamental question, Liu et al. [56] performed DFT based metadynamics simulations to scrutinize the reaction between H<sub>2</sub> and the prototypical FLP,

Table 1  
Experimentally examined combinations of Lewis acids (boranes) and Lewis bases (phosphines) with reactivity towards H<sub>2</sub> activation. *t*Bu = *tert*-butyl. Mes = 1,3,5-trimethylbenzene.

FLPs	Experimental results
1 <i>t</i> Bu <sub>3</sub> P + B( <i>p</i> -C <sub>6</sub> F <sub>4</sub> H) <sub>3</sub>	Nonreversible H <sub>2</sub> activation [6]
2 Mes <sub>3</sub> P + B(C <sub>6</sub> F <sub>5</sub> ) <sub>3</sub>	Nonreversible H <sub>2</sub> activation [65]
3 ( <i>o</i> -C <sub>6</sub> H <sub>4</sub> Me) <sub>3</sub> P + B( <i>p</i> -C <sub>6</sub> F <sub>4</sub> H) <sub>3</sub>	Reversible H <sub>2</sub> activation [65]
4 (C <sub>6</sub> F <sub>5</sub> ) <sub>3</sub> P + B(C <sub>6</sub> F <sub>5</sub> ) <sub>3</sub>	No reaction [6]
5 Mes <sub>2</sub> P(CH <sub>2</sub> ) <sub>2</sub> B(C <sub>6</sub> F <sub>5</sub> ) <sub>2</sub>	H <sub>2</sub> activation [43]
6 Mes <sub>2</sub> P(CH <sub>2</sub> ) <sub>3</sub> B(C <sub>6</sub> F <sub>5</sub> ) <sub>2</sub>	No reaction [43]
7 Mes <sub>2</sub> P(CH <sub>2</sub> ) <sub>4</sub> B(C <sub>6</sub> F <sub>5</sub> ) <sub>2</sub>	H <sub>2</sub> activation [43]

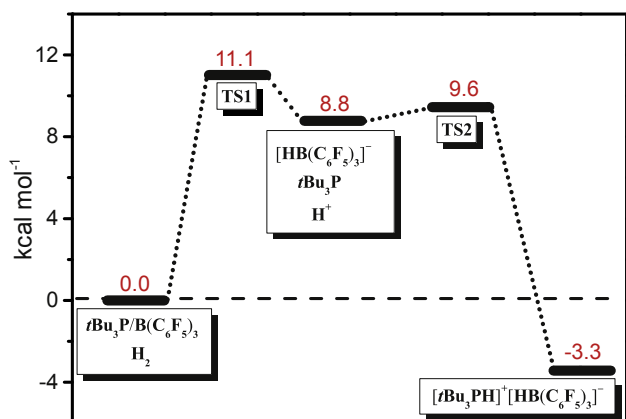


Fig. 1. One-dimensional free energy surface (1D FES) for the  $\text{H}_2$  activation by the FLP,  $t\text{Bu}_3\text{P}/\text{B}(\text{C}_6\text{F}_5)_3$ , obtained by metadynamics simulations.  $t\text{Bu}$  = *tert*-butyl.

$t\text{Bu}_3\text{P}/\text{B}(\text{C}_6\text{F}_5)_3$ . The free energy surface (FES) and the detailed reaction path for  $\text{H}_2$  activation by  $t\text{Bu}_3\text{P}/\text{B}(\text{C}_6\text{F}_5)_3$  (Fig. 1) showed that  $\text{H}_2$  activation by the  $t\text{Bu}_3\text{P}/\text{B}(\text{C}_6\text{F}_5)_3$  pair mainly consists of two elementary steps: hydride transfer to B and proton transfer to P, which is consistent with the previous AIMD studies [53–55]. An interesting insight is made on the individual roles of LA and LB [56]. On the one hand, the results showed that the  $\text{H}^-$  transfer to B has a much higher energy barrier than that of the  $\text{H}^+$  transfer to P (11.1 vs. 0.8  $\text{kcal mol}^{-1}$ ). The first step is endergonic, with a  $\Delta G$  of 8.8  $\text{kcal mol}^{-1}$  for the intermediate state, and an overall energy barrier is 11.1  $\text{kcal mol}^{-1}$  (the free energy difference between TS1 and the reactant) according to the energy span model [76]. These findings indicate that the  $\text{H}^-$  transfer is the rate-determining step. On the other hand, the  $\text{H}^-$  transfer step is strongly endergonic (8.8  $\text{kcal mol}^{-1}$ ), and the whole process becomes exergonic (−3.3  $\text{kcal mol}^{-1}$ ) when the  $\text{H}^+$  transfers to P. In short, the rate-limiting kinetics is determined by the LA, while the overall exergonic thermodynamics is determined by the LB.

### 3. Conclusions and outlook

Due to its clean and renewable properties, hydrogen is considered as a sustainable energy resource and is largely used for hydrogenation reactions of many different substrates. Along its line of usage, activation of  $\text{H}_2$  is the primary step, and FLPs have shown a promising capacity for this purpose.  $\text{H}_2$  activation by FLPs generally consists of the following steps: the Lewis acid and base components first associate to form an FLP complex with an optimal distance and orientation. After that,  $\text{H}_2$  enters the cavity of the FLP, and gets heterolytically polarized by the interactions with the two reactive centers in a two-step manner. Finally, the LA and LB components capture the hydride and the proton, respectively, forming the zwitterionic product. Generally, the more acidic and basic the two FLP components are, the lower the free energy barrier for  $\text{H}_2$  activation is, and the higher catalytic activity of the FLPs is. The stability of the final product also

depends on the strength of the FLPs. The overall kinetics is mainly affected by the strength of the LAs while the thermodynamics is more affected by the strength of the LBs. In addition, solvation effects also play a significant role for the  $\text{H}_2$  activation because the final hydrogenation product is often stabilized by the organic solvent.

Currently, FLPs reactivity is mainly investigated and applied in the solution phase, and most often the solvents are organic solvents. This might introduce certain environmental issues due to volatility of the aromatic organic solvents, and thus prevents the industrial applications of FLPs. These issues could be solved by incorporating the concept of FLPs into heterogeneous catalyst (e.g. molecular crystals), or by employing green solvents (e.g. ionic liquids). We may therefore expect to see in the near future the combination of FLP chemistry with green chemistry applications.

### Conflict of interest

There is no conflict of interest.

### References

- [1] H.C. Brown, H.I. Schlesinger, S.Z. Cardon, *J. Am. Chem. Soc.* 64 (1942) 325–329.
- [2] H.C. Brown, B. Kannerp, *J. Am. Chem. Soc.* 88 (1966) 986–992.
- [3] G. Wittig, E. Benz, *Chem. Ber.* 92 (1999) 1999–2013.
- [4] F. Developments, *Angew. Chem. Int. Ed.* 5 (1966) 351–371.
- [5] G.C. Welch, R.R. San Juan, J.D. Masuda, D.W. Stephan, *Science* 314 (2006) 1124–1126.
- [6] G.C. Welch, D.W. Stephan, *J. Am. Chem. Soc.* 129 (2007) 1880–1881.
- [7] C.M. Mömmling, E. Otten, G. Kehr, R. Fröhlich, S. Grimme, D.W. Stephan, G. Erker, *Angew. Chem. Int. Ed.* 48 (2009) 6643–6646.
- [8] I. Peuser, R.C. Neu, X. Zhao, M. Ulrich, B. Schirmer, J.A. Tannert, G. Kehr, R. Fröhlich, S. Grimme, G. Erker, D.W. Stephan, *Chem. Eur J.* 17 (2011) 9640–9650.
- [9] E. Otten, R.C. Neu, D.W. Stephan, *J. Am. Chem. Soc.* 131 (2009) 9918–9919.
- [10] M. Sajid, A. Klose, B. Birkmann, L. Liang, B. Schirmer, T. Wiegand, H. Eckert, A.J. Lough, R. Fröhlich, C.G. Daniliuc, S. Grimme, D.W. Stephan, G. Kehr, G. Erker, *Chem. Sci.* 4 (2013) 213–219.
- [11] A.E. Ashley, A.L. Thompson, D. O'Hare, *Angew. Chem. Int. Ed.* 48 (2009) 9839–9843.
- [12] S.D. Tran, T.A. Tronic, W. Kaminsky, D. Michael Heinekey, J.M. Mayer, *Inorg. Chim. Acta* 369 (2011) 126–132.
- [13] P. Chase, G.C. Welch, T. Jurca, D.W. Stephan, *Angew. Chem. Int. Ed.* 46 (2007) 8050–8053.
- [14] P. Spies, S. Schwendemann, S. Lange, G. Kehr, R. Fröhlich, G. Erker, *Angew. Chem. Int. Ed.* 47 (2008) 7543–7546.
- [15] S. Schwendemann, T.A. Tumay, K.V. Axenov, I. Peuser, G. Kehr, R. Fröhlich, G. Erker, *Organometallics* 29 (2010) 1067–1069.
- [16] D.W. Stephan, *Science* 354 (2016) aaf7229.
- [17] D.W. Stephan, G. Erker, *Angew. Chem. Int. Ed.* 49 (2010) 46–76.
- [18] D.W. Stephan, *Org. Biomol. Chem.* 10 (2012) 5740–5746.
- [19] T.A. Rokob, I. Pápai, *Top. Curr. Chem.* 332 (2013) 157–211.
- [20] B. Schirmer, S. Grimme, *Top. Curr. Chem.* 332 (2013) 213–230.
- [21] Z.X. Wang, L. Zhao, G. Lu, H. Li, F. Huang, *Top. Curr. Chem.* 332 (2013) 231–266.
- [22] T.M. Gilbert, *Top. Curr. Chem.* 332 (2013) 267–289.
- [23] D.W. Stephan, G. Erker, *Chem. Sci.* 5 (2014) 2625–2641.
- [24] D.W. Stephan, G. Erker, *Angew. Chem. Int. Ed.* 54 (2015) 6400–6441.
- [25] D.W. Stephan, *Acc. Chem. Res.* 48 (2015) 306–316.
- [26] J.M. Bayne, D.W. Stephan, *Chem. Soc. Rev.* 45 (2016) 765–774.



- [27] D.W. Stephan, *Top. Curr. Chem.* 332 (2013) 1–44.
- [28] C. Bannwarth, A. Hansen, S. Grimme, *Isr. J. Chem.* 55 (2015) 235–242.
- [29] G. Bistoni, A.A. Auer, F. Neese, *Chem. Eur. J.* 23 (2017) 865–873.
- [30] V. Sumerin, F. Schulz, M. Nieger, M. Leskelä, T. Repo, B. Rieger, *Angew. Chem. Int. Ed.* 47 (2008) 6001–6003.
- [31] A.J.V. Marwitz, J.L. Dutton, L.G. Mercier, W.E. Piers, *J. Am. Chem. Soc.* 133 (2011) 10026–10029.
- [32] T. Wiegand, M. Siedow, O. Ekkert, J. Möbus, C.G. Daniliuc, G. Kehr, G. Erker, H. Eckert, *Solid State Nucl. Magn. Reson.* 61–62 (2014) 8–14.
- [33] L. Rocchigiani, G. Ciancaleoni, C. Zuccaccia, A. Macchioni, *J. Am. Chem. Soc.* 136 (2014) 112–115.
- [34] T.A. Rokob, A. Hamza, A. Stirling, T. Soós, I. Pápai, *Angew. Chem. Int. Ed.* 47 (2008) 2435–2438.
- [35] S. Grimme, H. Kruse, L. Goerigk, G. Erker, *Angew. Chem. Int. Ed.* 49 (2008) 1402–1405.
- [36] L. Liu, N. Vankova, A. Mavrandonakis, T. Heine, G. Rösenthaller, J. Eicher, *Chem. Eur. J.* 19 (2013) 17413–17424.
- [37] M. Becerra, M.R. Enriquez, C.E. Gavilanes, *Theor. Chem. Acc.* 135 (2016) 1–11.
- [38] I. Bakó, A. Stirling, S. Bálint, I. Pápai, *Dalton Trans.* 41 (2012) 9023–9025.
- [39] C. Jiang, O. Blacque, H. Berke, *Organometallics* 28 (2009) 5233–5239.
- [40] M. Ullrich, A.J. Lough, D.W. Stephan, *Organometallics* 29 (2010) 3647–3654.
- [41] G. Kehr, S. Schwendemann, G. Erker, *Top. Curr. Chem.* 332 (2013) 45–83.
- [42] P. Spies, G. Erker, G. Kehr, K. Bergander, R. Fröhlich, S. Grimme, D.W. Stephan, *Chem. Commun.* (2007) 5072–5074.
- [43] T. Özgün, K. Ye, C.G. Daniliuc, B. Wibbeling, L. Liu, S. Grimme, G. Kehr, G. Erker, *Chem. Eur. J.* 22 (2016) 5988–5995.
- [44] K.V. Axenov, C.M. Mömming, G. Kehr, R. Fröhlich, G. Erker, *Chem. Eur. J.* 16 (2010) 14069–14073.
- [45] K. Ye, C.G. Daniliuc, S. Dong, G. Kehr, G. Erker, *Organometallics* 36 (2017) 5003–5012.
- [46] Y. Guo, S. Li, *Inorg. Chem.* 47 (2008) 6212–6219.
- [47] G.C. Welch, L. Cabrera, P.A. Chase, E. Hollink, J.D. Masuda, P. Wei, D.W. Stephan, *Dalton Trans.* 9226 (2007) 3407–3414.
- [48] L. Liu, P. Petkov, T. Heine, G. Rösenthaller, J. Eicher, N. Vankova, *Phys. Chem. Chem. Phys.* 17 (2015) 10687–10698.
- [49] P. Spies, G. Kehr, K. Bergander, B. Wibbeling, R. Fröhlich, G. Erker, *Dalton Trans.* (2009) 1534–1541.
- [50] S.M. Whittemore, G. Edverson, D.M. Camaioni, A. Karkamkar, D. Neiner, K. Parab, T. Autrey, *Catal. Today* 251 (2015) 28–33.
- [51] T. Özgün, K. Bergander, L. Liu, C.G. Daniliuc, S. Grimme, *Chem. Eur. J.* 22 (2016) 11958–11961.
- [52] R. Rajeev, R.B. Sunoj, *Chem. Eur. J.* 15 (2009) 12846–12855.
- [53] M. Pu, T. Privalov, *J. Chem. Phys.* 138 (2013) 154305.
- [54] M. Pu, T. Privalov, *ChemPhysChem* 15 (2014) 3714–3719.
- [55] M. Pu, T. Privalov, *ChemPhysChem* 15 (2014) 2936–2944.
- [56] L. Liu, B. Lukose, B. Ensing, *J. Phys. Chem. C* 121 (2017) 2046–2051.
- [57] A. Hamza, A. Stirling, T.A. Rokob, I. Pápai, *Int. J. Quant. Chem.* 109 (2009) 2416–2425.
- [58] B. Schirmer, S. Grimme, *Chem. Commun.* 46 (2010) 7942–7944.
- [59] D.M. Camaioni, B. Ginovska-pangovska, G.K. Schenter, S.M. Kathmann, T. Autrey, *J. Phys. Chem. A* 116 (2012) 7228–7237.
- [60] T.A. Rokob, I. Bakó, A. Stirling, A. Hamza, I. Pápai, *J. Am. Chem. Soc.* 135 (2013) 4425–4437.
- [61] D. Yepes, P. Jaque, I. Fernández, *Chem. Eur. J.* 22 (2016) 18801–18809.
- [62] D.W. Stephan, S. Greenberg, T.W. Graham, P. Chase, J.J. Hastie, S.J. Geier, J.M. Farrell, C.C. Brown, Z.M. Heiden, G.C. Welch, M. Ullrich, *Inorg. Chem.* 50 (2011) 12338–12348.
- [63] A.P. Lathem, B.L. Rinne, M.A. Maldonado, Z.M. Heiden, *Eur. J. Inorg. Chem.* 2017 (2017) 2032–2039.
- [64] T. Andra, A. Hamza, I. Pápai, *J. Am. Chem. Soc.* 131 (2009) 10701–10710.
- [65] M. Ullrich, A.J. Lough, D.W. Stephan, *J. Am. Chem. Soc.* 131 (2009) 52–53.
- [66] R.C. Neu, E.Y. Ouyang, S.J. Geier, X. Zhao, A. Ramos, D.W. Stephan, *Dalton Trans.* 39 (2010) 4285–4294.
- [67] C. Jiang, O. Blacque, T. Fox, H. Berke, *Dalton Trans.* 40 (2011) 1091–1097.
- [68] L. Liu, N. Vankova, T. Heine, *Phys. Chem. Chem. Phys.* 18 (2016) 3567–3574.
- [69] R.P. Bell, *Proc. R. Soc. A* 154 (1936) 414–429.
- [70] M.G. Evans, M. Polanyi, *Soc., Trans. Faraday* 34 (1938) 11–24.
- [71] L.E. Longobardi, L. Liu, S. Grimme, D.W. Stephan, *J. Am. Chem. Soc.* 138 (2016) 2500–2503.
- [72] T. Wang, G. Kehr, L. Liu, S. Grimme, C.G. Daniliuc, G. Erker, *J. Am. Chem. Soc.* 138 (2016) 4302–4305.
- [73] K. Ye, G. Kehr, C.G. Daniliuc, L. Liu, S. Grimme, G. Erker, *Angew. Chem. Int. Ed.* 55 (2016) 9216–9219.
- [74] K.L. Bamford, L.E. Longobardi, L. Liu, S. Grimme, D.W. Stephan, *Dalton Trans.* 46 (2017) 5308–5319.
- [75] L. Liu, J.G. Brandenburg, S. Grimme, *Philos. Trans. R. Soc. A* 375 (2017) 20170006.
- [76] S. Kozuch, S. Shaik, *Acc. Chem. Res.* 44 (2011) 101–110.